Curr Atheroscler Rep (2016) 18: 83
DOI 10.1007/s11883-016-0635-9

VASCULAR BIOLOGY (J. HAMILTON, SECTION EDITOR)

A Review on Atherosclerotic Biology, Wall Stiffness, Physics of Elasticity, and Its Ultrasound-Based Measurement

Anoop K. Patel[1] · Harman S. Suri[2] · Jaskaran Singh[1] · Dinesh Kumar[3] · Shoaib Shafique[4] · Andrew Nicolaides[5] · Sanjay K. Jain[1] · Luca Saba[6] · Ajay Gupta[7] · John R. Laird[8] · Argiris Giannopoulos[9] · Jasjit S. Suri[5,10,11,12]

Published online: 9 November 2016

Abstract Functional and structural changes in the common carotid artery are biomarkers for cardiovascular risk. Current methods for measuring functional changes include pulse wave velocity, compliance, distensibility, strain, stress, stiffness, and elasticity derived from arterial waveforms. The review is focused on the ultrasound-based carotid artery elasticity and stiffness measurements covering the physics of elasticity and linking it to biological evolution of arterial stiffness. The paper also presents evolution of plaque with a focus on the pathophysiologic cascade leading to arterial hardening. Using the concept of strain, and image-based elasticity, the paper then reviews the lumen diameter and carotid intima-media thickness measurements in combined temporal and spatial domains. Finally, the review presents the factors which influence the understanding of atherosclerotic disease formation and cardiovascular risk including arterial stiffness, tissue morphological characteristics, and image-based elasticity measurement.

Keywords Vascular · Atherosclerosis · Stiffness · Elasticity · Ultrasound · Tissue characterization · Risk stratification

This article is part of the Topical Collection on *Vascular Biology*

✉ Jasjit S. Suri
jasjit.suri@atheropoint.com

[1] Department of Computer Engineering, NIT, Kurukshetra, India

[2] Mira Loma, Sacramento, CA, USA

[3] Point-of-Care Devices, Global Biomedical Technologies, Inc., Roseville, CA, USA

[4] CorVasc Vascular Laboratory, Indianapolis, IN, USA

[5] Vascular Diagnostic Center, University of Cyprus, Nicosia, Cyprus

[6] Department of Radiology, University of Cagliari, Cagliari, Italy

[7] Radiology Department, Brain and Mind Research Institute, Weill Cornell Medical College, New York, NY, USA

[8] UC Davis Vascular Center, University of California, Davis, CA, USA

[9] Department of Vascular Surgery, Imperial College, London, UK

[10] Monitoring and Diagnostic Division, AtheroPoint™, Roseville, CA, USA

[11] Department of Electrical Engineering, University of Idaho (Affl.), Moscow, ID, USA

[12] Diagnosis and Stroke Monitoring Division, AtheroPoint™, Roseville, CA, USA

Introduction

Cardiovascular diseases (CVDs) are the main cause of worldwide mortality and morbidity [1]. Around 30% of the deaths in western countries are due to CVD [2]. Early diagnosis of CVD is necessary to avoid the risk of mortality [3]. One of the leading causes of the development of CVD and stroke is atherosclerotic disease [4]. Simply put, this is a buildup of fatty material known as plaque in arterial walls, leading to the narrowing of the arteries. To improve our ability to diagnose, monitor, and treat atherosclerosis, it is necessary to understand the biology of the endothelial layer and its implications on the formation of plaque. For example, as the permeability of the endothelium increases, more molecules are able to penetrate which eventually leads to the biochemical cascade resulting in plaque formation. Thus, the first section of the paper lays the groundwork for the rest of the paper for better understanding of the basic biology of atherosclerosis prior to discussing imaging strategies to detect the disease and to monitor its evolution.

Arterial stiffness was found to be associated with atherosclerosis [5•]. In order to predict the risk of CVD, stiffness is one of the primary factors useful to consider [6]. Because arterial stiffness has been shown to be a useful biomarker for CVD [7] and due to technical challenges involved in noninvasively assessing arterial stiffness, this paper analyzes the biology and causes of stiffness. Several studies have been performed to predict CVD risk based on arterial stiffness [8, 9]. Our review aims to link different concepts central to atherosclerosis including the evolution of arterial stiffness and grayscale imaging of carotid arteries in an attempt to lead to an improved understanding of imaging-based elasticity measurements to aid in stroke/CVD risk stratification.

An additional method for risk stratification of CVDs is through the evaluation of image-based arterial parameters, such as the link between carotid intima-media thickness (cIMT) and arterial stiffness which has been shown to be powerful in diseased versus control groups [7]. The arterial stiffness increases with the increase in IMT [10]. The current method of elasticity computation relies on the arterial parameter of PWV [11, 12]. However, PWV is based on waveforms which are not accurate due to stiffness variations in the artery throughout the length it is measured [13]. Therefore, this paper talk about the Young's modulus of elasticity (YEM) in terms of IMT and lumen diameter (LD) [14], the two arterial parameters using the basic concepts of ratio of stress to strain.

The layout of this paper is as follows: the biology of the atherosclerosis disease is presented in "Biology of Atherosclerosis Disease and Evolution of Arterial Stiffness" section, demonstrating the stages of plaque formation along with the concept of arterial stiffness and its evolution. The assumptions for risk stratification for CVD and the arterial parameters are discussed in "Hypothesis: A Link between Plaque Morphology, Elasticity and Measurements" section. The physics of elasticity and its measurements is discussed in "Physics of Elasticity and its Measurements" section, while the overview of imaging-based solutions is presented in "Overview of IMT/LD Delineation Methods" section. The detailed discussions are presented in "Discussions" section, and the paper concludes in "Conclusions" section.

Biology of Atherosclerosis Disease and Evolution of Arterial Stiffness

Atherosclerosis and Its Causes The fundamental cause of stroke or cardiac arrest is due to a disease called atherosclerosis [4]. In atherosclerosis, plaque develops and hardens over time inside the walls of the arteries. Atherosclerosis may be caused by a number of factors such as: (1) an atherogenic diet, having cholesterol and structural fat in excess; (2) leukocyte accumulation; healthy endothelium do not have an adhesive nature with leukocytes, but after the initiation of hypercholesterolemia, the endothelium becomes adhesive [15]; (3) damaging of the endothelium in arterial walls [16]. These causes of atherosclerosis start changing the parameter of the artery such as IMT and LD.

Types of Leukocyte Penetrating Intima Layer The presence of some specific types of leukocyte adhesion molecules on the endothelium cell attracts monocytes and T-cells towards the endothelium. The monocytes deposited at endothelium penetrate the intima layer and can consume lipid and become foam cells or lipid laden macrophages. Some cells however, which are classical surface receptors for low density lipoproteins (LDL), do not become foam cells. Complex plaques are formed when these monocytes move towards the intima layer while smooth muscle cells (SMCs) move towards the endothelial layer.

Endothelium Layer One of the fundamental causes of plaque formation is damage to the endothelium. This happens due to extreme interactions between two types of white blood cells (or leukocytes): monocytes and T-lymphocytes. Monocytes and T-lymphocytes interact with the endothelium in order to enter into the artery wall [17]. The permeability of the endothelium is the first to change during the process of plaque buildup (Fig. 1b). Because of this, increased amounts of lipoprotein are transported by the endothelium and placed in the sub-endothelial space of the intima layer. The composition of the extra cellular matrix below the endothelium attracts and promotes the coagulation of cholesterol containing LDL particles in arterial walls [18]. These LDL particles promote the process of atherosclerotic plaque building and are analogous to plasminogens that make the extracellular matrix prothombotic in nature [19].

Plaque and Fibrous Cap Formation Plaque development also involves the engagement and movement of SMCs from the media layer to the intima layer (Fig. 1c) [20••]. SMCs, which are present in media layer (Fig. 1a), migrate into the intima layer and form a bulk of the auxiliary cellular matrix. This is known as the process of plaque development [21]. The SMCs moved from the media layer are also able to reach the surface and create a layer called the fibrous cap [17]. The fibrous cap has an elastic property, which keeps it safe from rupturing. However, as it stiffens the possibilities of rupture increases. SMCs that move from the media to intima layer are broken by inflammatory cells. Thus, the cap is strengthened and becomes more stable. The stiffness index of the cap can determine the possibility of the rupture of the plaque. So, it is important to find the stiffness for the risk assessment of the stroke.

Effect of Plaque Formation on Blood Vessels Blood pressure creates a stress on the artery that decreases the force-

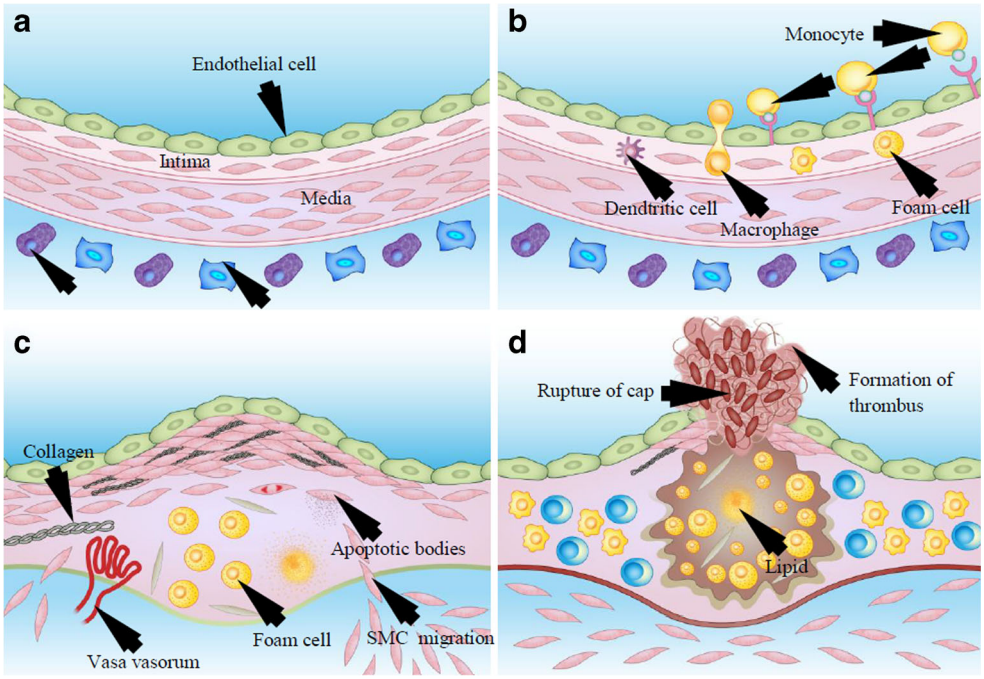

Fig. 1 Stages for development of atherosclerotic plaque lesions (courtesy of AtheroPoint, Roseville, CA, USA)

bearing capacity of the fibrous cap over time, leading to a great risk of rupturing (Fig. 1d) [22]. The material properties of the media, fibrous cap, lipid, and intra-plaque hemorrhage/thrombus from human carotid atherosclerosis plaque exhibit a non-linear behavior, with an increased stiffness while stretched [23]. The risk can be stratified with the help of the analysis of stiffness and elasticity of the artery discussed in "Overview of IMT/LD Delineation Methods" section.

Arterial Stiffness The accumulation of lipid in the vessel artery over time leads to the calcification and formation of plaque. Rupture of this plaque then leads to the formation of clots and acute morbid events [24]. Initially, plaque development starts with the deposition of small lipid and fatty materials in the intima, which may develop into complex plaque structures over the time. Advanced plaque has a heterogeneous composition that includes a lipid core, calcification and fibrous connective tissue deposits. The increased stiffness of the large arteries due to atherosclerotic disease is a useful biomarker for CVD.

Cause of Arterial Stiffness Cellular fibrosis is the topmost layer of atherosclerotic plaque that contains the SMCs. The elastic property of SMCs determines the amount of force the arterial wall can withstand [25]. The major contribution in vascular stiffness is from SMCs which line the interior of vascular walls [26]. Elimination of the SMCs present in an artery, during the replication process, prevents the formation of atherosclerotic plaque. The small number of SMCs that are present in an advanced atheroma breaks into deoxyribonucleic acid (DNA), that leads to programmed cell death, or apoptosis [26, 27]. As the atheroma evolves inside the artery, the inflammatory cytokines causes apoptosis, which also support the death of SMCs [28]. The accumulation of SMCs is probably the result of cell death and replication, which leads to the stiffness of the artery. Arterial stiffness also increases with the age. Another study was given that shows other causes of the increase of stiffness, i.e., change in the ratio of collagen and elastin present in the extracellularmatrix of the arterial media [29].

Hypothesis: a Link between Plaque Morphology, Elasticity, and Measurements

The risk of CVD can be analyzed by using plaque components or arterial parameters. The parameters that can predict the risk factors of CVDs include arterial elasticity, stiffness, LD, and IMT. We are presenting the link between (a) these plaque components leading to the arterial stiffness and (b) relationship of IMT to arterial stiffness in the forthcoming subsections.

Link between Plaque Components and Carotid Stiffness

The biological evolution of stiffness section strongly supports that the plaque components are responsible for arterial stiffness which leads to the risk of CVD. Several authors showed the application of stiffness in stratification of patients into diseased and control groups [30–32]. These authors showed that the arterial stiffness in (i) type-2 diabetes [9], (ii) Kawasaki [30] and (iii) beta thalassaemia major [31] patients was higher

compared to the control group. These evidences showed that the stiffness of plaque can be used for risk stratification of patients into the high risk category. Thus, it leads us in the direction for better understanding, that the changes in the plaque components have a direct link to stiffness.

Link between cIMT and Carotid Stiffness

Carotid IMT and Stiffness The change in arterial stiffness is due to the change in structural and functional components of artery [8]. These changes in structure and functional properties of vessel wall also cause the cIMT to change which is one of the key biomarkers for CVD [8, 33••]. The potential cause of the change in cIMT starts from the fracture of elastin, hike in collagen and deposition of calcium inside the artery [34]. On the basis of the literature discussed so far, we can classify the methods into two sets of studies: (a) studies where changes in IMT are used for stratification into normal and abnormal groups and (b) studies where IMT and stiffness are jointly used for stratification [10]. In class (a), several authors showed that there was an increase in the IMT of the diseased group compared to the control group [8, 33••]. In class (b), several authors have contributed demonstrating the changes in both the IMT and stiffness of the artery [30–32, 35] and it was seen higher in the diseased group (beta thalassaemia major disease, Kawasaki disease, type-2 diabetes disease and cerebral small vessel disease) compared to the controlled group. This clearly shows that the diseased group and control group can be stratified on the basis of changes in both IMT and arterial stiffness. We conclude from the above discussions that IMT and carotid stiffness both undergo changes and can be used to discriminate between diseased and control groups.

Physics of Elasticity and Its Measurements

The most common methodology to represent the arterial elasticity is in terms of waves. The wave is represented by the blood movement which travels from one region of the body to another region, and the velocity of the wave is called Pulse Wave Velocity (PWV) [11, 12, 36]. YEM is shown to have relationship with PWV. The second method of elasticity evaluation takes into account the imaging-based characteristics of the arterial physical structures in spatial and temporal domains [37, 38].

Young's Modulus of Elasticity in Terms of Pulse Wave Velocity

If the time instance at which the pressure wave arrives at carotid and femoral arteries are represented by t_1 and t_2, respectively and Δt is the difference between the time instances: $\Delta t = t_2 - t_1$, then the *PWV* is mathematically given as Eq. 1 of the Appendix A. Arterial elasticity can be computed using *PWV* which is measured by a reference wave in the electrocardiogram [36]. This *PWV* parameter has shown to have an association with CVD [11, 12, 36, 39]. *PWV* is commonly expressed using YEM, the density of fluid within the lumen, and lumen radius [40] and is given as Eq. 2 of the Appendix A. Thus, Young's elastic modulus Y_m is expressed as Eq. 3 of Appendix A. The estimated young's modulus of the elasticity in terms of PWV talks about the elasticity of the artery in a defined length. Note that Y_m is not uniform throughout the length [13].

Young's Modulus of Elasticity in Terms of Arterial Diameter and Intima-Media Thickness

YEM is defined as a mechanical property of linear elastic material. This can be expressed as the ratio of stress to strain. The objective of this section is to derive YEM in terms of LD and IMT. Let *PP* be the pulse pressure, i.e., the difference between systolic blood pressure (P_s) and the diastolic blood pressure (P_d), given as: $PP = (P_s - P_d)$. Correspondingly, let *DD* be the strain and is mathematically given in Eq. 4 of the Appendix A. The Peterson's elastic modulus (E_p) can be mathematically given as the ratio of PP to DD in Eq. 5 of the Appendix A. Arterial distensibility (DIS) is a reciprocal of E_p and is mathematically given as: $\frac{1}{E_p}$.

Circumferential stress of the artery in terms of *PP*, minimum arterial diameter and IMT during minimum arterial diameter was recently shown by Soleimani et al. (2015) [38] and is given as in Eq. 6. Young's elastic modulus (Y_m) is defined as the ratio of stress to strain and can also be derived in terms of *PP, DD*, D_{min} and $IMT_{D_{min}}$, by substituting σ_{cs} in the Eq. 3 of the Appendix A, we get Y_m as in Eq. 7 of the Appendix A. Y_m can also be expressed in terms of Peterson's elastic modulus (E_p) as given in Eq. 8 of the Appendix A.

Compliance and Distensibility

Radial Compliance Compliance and distensibility are two measurements used to predict the risk of CVD based on pulse pressure and maximum and minimum arterial diameter [33••]. Arterial compliance is defined as the change in volume of the blood in artery with the change in pressure. Radial compliance coefficient (CC_r), is the ratio of, difference of square of maximum and minimum diameter of artery, and *PP* and given as in Eq. 9 of the Appendix A.

Arterial Distensibility It is the ratio of DD_{sr} to *PP*, where DD_{sr} is defined as the ratio of the difference of the square of maximum diameter and minimum diameter of artery to square of minimum diameter. It is mathematically stated as in Eq. 10 of the Appendix A. Using above approach elasticity is

calculated and data were compared for two consecutive cardiac cycles and they have almost a linear relation.

Volumetric Compliance It was hypothesized that radial stress and radial strain were due to changes in blood pressure [33••]. The radial compliance did not consider the longitudinal stress and longitudinal strain [41]. Recently, it was shown that longitudinal movement in the artery during the cardiac cycle can be used as a biomarker of CVD [42]. The concept of combining the radial and longitudinal stress/strain will lead to the evolution of volumetric compliance unlike considering only radial component alone.

Volumetric compliance coefficient (CC_v) can be mathematically defined in terms of arterial diameters, length of artery considered for volume measurement and pulse pressure. The estimation of diastolic length (L_d) and systolic length (L_s) is a challenging task in order to calculate volumetric compliance coefficient. The mathematical expression of CC_v is given in Eq. 11 of the Appendix A. These diameters used in Eq. 11 can be computed either using Doppler shift method by utilizing the mass of conservation principle [43, 44] or imaging-based method presented in "Overview of IMT/LD Delineation Methods" section.

Overview of IMT/LD Delineation Methods

The delineation of (i) lumen-intima (LI) and media-adventitia (MA) interfaces and (ii) near and far intima walls is one of the primary requisites for elasticity computation in an image-based paradigm. This delineation can be thought of as a segmentation process using image analysis and such a paradigm can be divided into four different segmentation categories (i) region-based, (ii) edge-based, (iii) fusion-based, and (iv) tracking and registration-based. An overview of these methods is provided in this section.

Region-Based Approaches

Fundamental concept in a region-based method is to extract the boundaries between the regions based on the discontinuities and statistical properties of the regions. These regions in an image are the set of connected pixels with homogenous properties such that each pixel in the image belongs to a definite region. There are three basic approaches adapted for region-based segmentation: (i) region growing, (ii) region splitting, (iii) combined region-splitting and merging [45].

The region of the arterial wall can also be segmented based on statistical models using certain assumptions. Destrempes et al. (2009) proposed a segmentation algorithm based on Nakagami distribution and stochastic optimization for motion image frames [46]. Under special constraints, Nakagami can be used for deriving the Rayleigh distribution, which can be then adapted to model the segmentation process [47]. This algorithm used a Bayesian classification model for segmentation followed by delineation of LI/MA interfaces and eventually IMT measurement [48]. Several other authors have delineated the LI/MA far wall borders in temporal frames [49–52]. The scope of this study is limited, and readers are recommended to explore all engineering-based methods in the above mentioned citations.

Edge-Based Approaches

In the edge-based segmentation, it is defined using discontinuities in the homogeneity and the segmentation is modeled with intensity profiles. Edges can be classified into step, line, ramp or a roof on the basis of the type of intensity transition. Typically, the edge-based segmentation has three basic steps as (i) noise reduction by smoothing, (ii) initial edge point detection (using processing operator [53]), and(iii) fine tuning the initial edge points to optimized edge positions. The edge-based methods can be categorized into several types: deformable model, direction-based, dynamic programming, and edge-linking. Deformable models were attempted by several authors for LI/MA delineation [54–56]. This model is based on the energy minimization approach and has shown to have good performance on noisy image. Directional-edge based method is advantageous when we are segmenting a pattern of intensities of the plaque. Molinari et al. (2011) used it for wall segmentation while moving from MA to LI [57]. Hough transform is typically adapted for line and circle detection and was used for common carotid artery (CCA) segmentation [58]. Dynamic programming was used by Liang et al. (2000) for connecting the broken edges [59]. Edge-linking is typically adapted when the noise levels are high and when the initial borders are disconnected [60]. Gradient-based approaches have also been adopted for segmentation of CCA in a static frame [60]. Static edge-based methods for LI/MA detection and IMT/LD measurement can be extended to carotid cine-loops [61–64]. All the above methods have two steps in common: (a) carotid recognition phase followed by (b) LI/MA detection in the recognized phase [65]. For further details, see the reviews by Suri's team [66•].

Fusion-Based Approaches

Fusion-based methods are the one which combines pixel-classification strategies with edge-based methods. Suri's team has used several such methods where the guidance zone is estimated using classifiers in the ROI and then used edge-based models like FOAM for LI/MA interface extraction [67]. Thus, the two-stage process of pixel-classification and edge extraction can be considered as a fusion of two different techniques. Such models are more accurate, but can be time-consuming due to heavy number crunches and an iterative

paradigm [68, 69]. Another approach in fusion method is combining different boundary-based methods such as greedy techniques for fusion of two techniques to obtain results closer to the goal state [70]. Hassan et al. (2014) had proposed fuzzy c-mean-based carotid wall segmentation and measured IMT value [71]. Static image segmentation using random sample consensus was proposed that uses cubic splines [72]. These static methods can be extended to the motion image frames.

Tracking and Registration Approaches

Tracking is the process of extracting corresponding features in successive frames of a video sequence. The tracking of LI/MA interfaces was adapted by considering radial movement [33••, 38]. Echo-tracking method has been shown for tracking the LI/MA edges during the longitudinal and radial motion of the carotid artery [73]. Image registration was also used to track the LI/MA edges [74]. This technique maps the high intensity LI/MA edge information of one image frame to edge information in the neighboring frames. IMT and LD were estimated followed by calculation of arterial stiffness using echo-tracking methodology [9, 75]. This method was used for estimation of subtle movement in the artery. Apostolakis et al. (2012) has proposed the tracking algorithm for motion data in a cardiac cycle [76].

A Note on Distance Metrics IMT measurement or LD measurement requires a stable metric or a ruler for measurement. The measurement of the distance between two tracked edges (LI/MA or LI near/LI far) has number of approaches [77]. Some of the approaches are as follows: polyline distance measurement [78], Housdrorff distance measurement [79], centerline distance measurement [77], Euclidean distance measurement, and morphological distance measurement. These methods provide the potential for accurate measurement of IMT and LD.

Discussions

Biology, Arterial Stiffness, Internal and External Factors Arterial stiffness is the consequence of the biological changes in artery (Section 2), which in turn leads to the change in the wall structure. These walls further undergo mechanical changes due to blood pressure. There are two kinds of forces present in the arterial wall: (a) one responsible for transverse strain, derived by intra-luminal pressure; (b) shear stress, due to the movement of the blood. These cause the changes in arterial stiffness [80]. Due to changes in arterial stiffness, there are changes in arterial parameters like compliance, augmentation index [81]. Arterial stiffness is affected by both internal and external factors (Fig. 2). We briefly discuss them here.

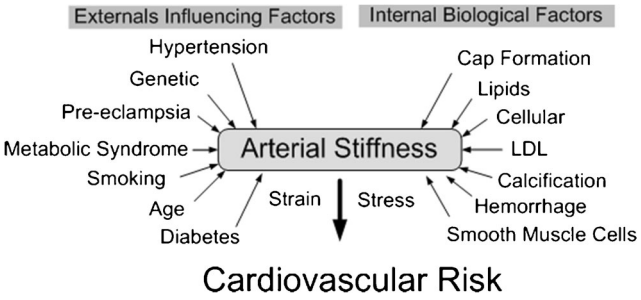

Fig. 2 External and internal factors affecting the arterial stiffness

Internal Biological Factors A biochemical change causes the changes in arterial stiffness. The internal biological factors which make an artery stiffen are: Cap formation [23, 82], lipid formation [23, 25, 83], cellular growth of the atherosclerotic disease [24], LDL [18, 19], calcification [84], hemorrhage [23], and SMC formation [20••, 25–27, 85].

External Influencing Factors There are many influencing factors such as age, diabetes, blood pressure (hypertension), pre-eclampsia, genetics, and smoking that affect the arterial stiffness over time (Fig. 2). Arterial stiffness is shown to have a positive correlation with age [22, 34, 86]. Arterial stiffness is also associated with blood pressure and increases in patients with hypertension without changing the structure of artery [27, 87]. Patients with diseases such as type-2 diabetes and pre-eclampsia have shown an increase in stiffness over time [8, 9, 15, 88]. Several authors have shown the effect of genetic factors on arterial stiffness [89•]. Smoking has also shown to have a relationship with stiffness and this stiffness remains after cessation of smoking [90].

Engineering Parameters, Methods, and Its Validation Due to the risk prediction ability of IMT and LD during the cardiac cycle, these parameters are of prime importance [91]. Wall (LI/MA) delineation in frozen frames has been extensively studied by Suri's team [49]. Motion data provides the temporal information [92] and Table 1 shows the benchmarking table listing the authors who have contributed in the image analysis area that finds the IMT/LD in cardiac cycle. There are two important axioms on edge-tracking methodology that must be satisfied for evaluating the arterial parameter [73]: (i) the artery can be considered in motion if one of the walls (near or far) is in motion during the cardiac cycle; (ii) there is a movement of the interface (say LI) if the surrounding walls undergoes changes (say in lumen and media wall). Currently, no cross validation of elasticity measurement of arterial wall has been done [33••, 38, 93, 94].

A Note on Risk Assessment Risk assessment is the process of characterizing possible future risk of disease. IMT is a possible measure of subclinical atherosclerosis at its earliest form [95]. Arterial stiffness is directly associated with risk of CVD

Table 1 Benchmark of automatic IMT techniques

SN	Authors	Technique	Artery	Patient Size	Frame per video	Validation	Performance
1	Destrempes et al. 2009 [46]	1. A semi-automatic model based on the distribution using disease free patients. 2. It uses mixture of three Nakagami distributions for modeling ROI having IMC. 3. Estimation of Maximum a Posterior distribution is offline.	CCA	15	20	Manual tracings and variability study For CCA: LI error (GT_1, GT_2) = 0.22 ± 0.11 mm MA error (GT_1, GT_2) = 0.15 ± 0.05 mm	Mean IMT = N/A For CCA: LI Error (GT1) = 0.21 ± 0.13 mm MA Error (GT1) = 0.16 ± 0.07 mm LI Error (GT2) = 0.18 ± 0.11 mm MA Error (GT2) = 0.15 ± 0.10 mm
			ICA			For ICA: LI error (GT_1, GT_2) = 0.33 ± 0.17 mm MA error (GT_1, GT_2) = 0.40 ± 0.29 mm	For ICA: LI Error (GT1) = 0.32 ± 0.14 mm MA Error (GT1) = 0.33 ± 0.22 mm LI Error (GT2) = 0.32 ± 0.18 mm MA Error (GT2) = 0.33 ± 0.23 mm
2	Apostolakis et al. 2012 [76]	1. A computerized motion analysis method is proposed that uses weighted-least squares optical flow (WLSOF) method. 2. The ROI containing far-wall is defined manually. 3. Strain elastograms is defined using the displacement during cardiac cycle.	CCA	3	25	N/A	Mean IMT = N/A
3	Kanber et al. 2012 [62]	1. Computerized Tracking of the arterial lumen based on probabilistic Approach. 2. Neighboring pixel of the ROI is related with the dependency of Gaussian relationship.	CCA	1	90	Benchmark against Region growing algorithm and Ver nier caliper measurement	Mean IMT = N/A P.T. = 33 m. second/frame
5	Ilea et al. 2013 [61]	1. Fully automatic model-based segmentation based on Adaptive Normalized Correlation tracking. 2. The ROI containing the IMC is modeled using canny edge detector and slope intercept.	CCA	23	40	Manual tracings	Mean IMT = 0.60 ± 0.10 mm
6	Chen et al. 2014 [63]	1. A fully automated algorithm estimation and identification of IMT. 2. LI interface and MA interface of posterior wall is detected automatically using gradient based method, respectively. 3. Canny edge detectoris used for getting candidate points.	CCA	13	06	Benchmarks against Ilea et al. 2013 [61] Molinari et al. 2012 [78]	Mean IMT = 0.61 ± 0.085 mm
7	Menchon-Lara et al. 2014 [51]	1. Automatic segmentation model for the IMT measurement. 2. Segmentation uses pattern recognition, and a combination of trained artificial neural networks.	CCA	30	–	Manual tracing	IMT Error = .03763 ± .02528 mm LI interface Error = .03703 ± .01857 mm MA interface Error = .03452 ± .01029 mm
8	Zahnd et al. 2014 [92]	1. Automatic derivation of the IMT from contours. 2. It uses the combination of shape-adapted filter bank and an innovative spatial transformation.	CCA	82	26	Benchmark against The Mann-Whitney *U* test. Total amplitude of the IMT variation.	IMT Error = .022 ± .016 mm LI interface Error = .029 ± .027 mm MA interface Error = .042 ± .038 mm
9	Carvalho et al. 2015 [52]	1. Fully Automatic model-based segmentation using intensity joint-histogram classification and graph model. 2. Nonrigid motion estimation to estimate the nonrigid deformation of the CA over time. 3. Distensibility measurement of CA.	CCA	DS1: 9 DS2: 8	11 10	Benchmarked against Standard result	Mean IMT = N/A IMT Error (DS1) = 0.19 ± 0.043 mm IMT Error (DS2) = 0.35 ± 0.176 mm

[96] and increase in stiffness may increase the risk of CVD. With the above discussion, the assessment of stiffness is directly associated with the assessment of the risk of CVD. IMT and LD may indirectly provide insight into stiffness, and these parameters are themselves able to predict the risk of CVD.

Limitations of Surrogate Makers and Steps Towards Improving the Clinical Outcomes

Limitations Elasticity of the arterial wall is an independent predictor of CVD, but the evaluation of an accurate value of elasticity is a challenging task. Surrogate markers like IMT, arterial lumen diameter for static and motion data during the cardiovascular cycle has a great relevance for early disease monitoring [97]. The accuracy of the stiffness value may be improved by using dynamic data collected during the heart cycle or by using other imaging modalities. These surrogate markers have some limitations such as they lack the characterization to evaluate the atherosclerotic disease. Further, these markers need to be tracked accurately over time which is currently not available conventionally. Lastly, these surrogate markers need to be computed automatically, reliably, and in a telemedicine-based paradigm [98] thereby improving the healthcare costs and infrastructure. Multimodality imaging can be adapted to improve the validation of the surrogate markers. Machine learning approaches can be adapted for disease characterization thereby utilizing these surrogate markers.

Steps for Improving the Clinical Outcomes Application of these surrogate markers can be converted to clinical outcomes by undergoing mini clinical trials with varying degree of input ultrasound acquisition digital imaging parameters such as frequency, image resolutions, parameters like compound and harmonic imaging, dynamic range and gain control. These parameters can be collected over large number of OEM ultrasound machines and scanning performed over large populations with varying degree of atherosclerotic disease severity. Such databases can be built and algorithms of surrogate markers can be further validated clinically and even histologically. These combined efforts can be developed for better clinical outcomes.

Conclusions

This paper presented a comprehensive review for understanding ultrasound-based elasticity for cardiovascular risk stratification by analyzing 98 citations selected based on quality and relevance. The paper first presented the biological evolution of atherosclerosis for better understanding of arterial stiffness.

The carotid plaque components and their role for imaging-based elasticity were used as a link in our novel review. The review presented the physics of arterial elasticity followed by imaging-based lumen diameter and carotid intima-media thickness measurement, given the cardiac cycle's spatial and temporal frames of the B-mode carotid ultrasound. Different image-based techniques for diameter, wall thickness, covering its basic concepts, pros-and-cons were discussed and analyzed. Further work is needed to link such methods to a multi- modality framework for elasticity validation.

Contributions Anoop K. Patel, MTech: Design of the manuscript pursing doctoral degree.

Harman S. Suri: Support in the design of the manuscript.

Jaskaran Singh, BTech: Support in the design of the manuscript.

Dinesh Kumar, PhD: Support in the design of the manuscript.

Shoaib Shafique, MD: Supported in clinical application and risk scores.

Andrew Nicolaides, PhD: Clinical advisor and discussions on carotid imaging.

Sanjay K. Jain, PhD: Advising and support in arranging information technology resources.

Luca Saba, MD: Clinical discussions and data collection.

Ajay Gupta, MD: Input in stroke and clinical component of the manuscript.

John R. Laird, MD: Clinical advisor for link between carotid and coronary.

Argiris Giannopoulos, MD; AVI carotid cine loop collection, demographics and library support.

Jasjit S. Suri, PhD, MBA, Fellow AIMBE: Principal Investigator of the project.

Compliance with Ethical Standards

Conflict of Interest Jasjit S. Suri (PI of this project) has a relationship with AtheroPoint™, Roseville, CA, USA which is dedicated to Atherosclerosis Disease Management, including Stroke and Cardiovascular imaging.

Anoop K. Patel, Harman S. Suri, Jaskaran Singh, Dinesh Kumar, Shoaib Shafique, Andrew Nicolaides, Sanjay K. Jain, Luca Saba, Ajay Gupta, John R. Laird, and Argiris Giannopoulos declare that they have no conflict of interest.

Human and Animal Rights and Informed Consent This article does not contain any studies with human or animal subjects performed by any of the authors.

Appendix A

$$PWV = \frac{d}{t_2 - t_1} = \frac{d}{\Delta t}, \tag{1}$$

where d is the distance measured between carotid to femoral arterial sites.

$$PWV = \sqrt{\frac{IMT \times Y_m}{2 \times \rho \times r}}. \tag{2}$$

Thus, Young's elastic modulus Y_m is expressed as:

$$Y_m = \frac{\left(2 \times \rho \times r \times PWV^2\right)}{IMT} \tag{3}$$

where *IMT* Y_m, ρ and r are intima-media thickness, YEM, density of fluid within the lumen and lumen radius, respectively.

$$DD = \left(\frac{D_{\max} - D_{\min}}{D_{\min}}\right), \tag{4}$$

where $D_{\max}$ is the maximum artery diameter and $D_{\min}$ is the minimum artery diameter.

Peterson's Elastic Module (E_p) can be expressed as:

$$E_p = \frac{PP}{DD}, \tag{5}$$

where PP is the pulse pressure and DD is the as in Eq. (4).

$$\sigma_{cs} = \frac{PP \times D_{min}}{2 \times IMT_{D_{min}}}, \tag{6}$$

where σ_{cs} is the circumferential stress, $IMT_{D_{min}}$ is the IMT measured at the instance when arterial diameter was minimum in the far wall.

$$Y_m = \frac{\text{Stress}}{\text{Strain}} = \frac{\sigma_{cs}}{DD} = \frac{\left[\frac{PP \times Dmin}{2 \times IMT_{D_{\min}}}\right]}{DD} = \left[\frac{PP}{DD}\right] \times \left[\frac{D_{\min}}{2 \times IMT_{D_{\min}}}\right] \tag{7}$$

If $E_p = \frac{PP}{DD}$ (Peterson's elastic modulus), then Y_m can be expressed in terms of Peterson's elastic modulus (E_p) as:

$$Y_m = \frac{E_p \times D_{\min}}{2 \times IMT_{D_{\min}}}. \tag{8}$$

$$CC_r = \frac{\left(D^2_{\max} - D^2_{\min}\right)}{PP}. \tag{9}$$

Distensibility DIS can be represented as:

$$DIS = \frac{DD_{sr}}{PP} = \frac{CC_r}{D^2_{\min}}, \tag{10}$$

where $DD_{sr} = \left[\frac{\left(D^2_{\max} - D^2_{\min}\right)}{D^2_{\min}}\right]$, PP is the pulse pressure; $D_{\max}$ is the maximum diameter of artery and $D_{\min}$ is the minimum diameter of artery.

$$CC_v = \frac{\pi}{4PP} \times L_d \times \left(D_s^2 - D_d^2\right) + \frac{\pi}{4PP} \times L_d \times D_s^2 \times \frac{\Delta L}{L_d}. \tag{11}$$

where, $\frac{\Delta L}{L_d}$ is expressed in terms of *IMT*, LD and arterial compressibility. It is mathematically represented as in Eq. 12:

$$\frac{\Delta L}{L_d} = \left[(1-\delta) \times \frac{IMT_d \times (D_d + IMT_d)}{IMT_s \times (D_s + IMT_s)}\right] - 1 \tag{12}$$

and L_d, D_s, D_d, PP, δ, IMT_d, and IMT_s are diastolic length of cylindrical artery, systolic diameter, diastolic diameter, pulse pressure, compressibility factor, diastolic *IMT* and systolic *IMT*, respectively. δ can be expressed as:

$$\delta = 1 - \frac{V_s}{V_d}, \tag{13}$$

where V_d and V_s is volume of vessel wall in diastole, systole, respectively. V_s and V_d can be computed using Eq. 14 as:

$$\begin{cases} V_s = \pi \times L_s \times IMT_s \times [D_s + IMT_s] \\ V_d = \pi \times L_d \times IMT_d \times [D_d + IMT_d] \end{cases} \tag{14}$$

where L_s is the systolic length of cylindrical artery, D_s and D_d are the diastolic and systolic diameter, respectively.

References

Papers of particular interest, published recently, have been highlighted as:
- • Of importance
- •• Of major importance

1. Mozaffarian D, Benjamin EJ, Go AS, Arnett DK, Blaha MJ, Cushman M, et al. American Heart Association Statistics Committee and Stroke Statistics Subcommittee. Heart disease and stroke statistics—2015 update: a report from the American Heart Association. Circulation. 2015;131:29–322.
2. Pagidipati NJ, Gaziano TA. Estimating deaths from cardiovascular disease: a review of global methodologies of mortality measurement. Circulation. 2013;127:749–56.
3. Schmidt R, Lauter J. MyHeart: fighting cardio-vascular diseases by preventive lifestyle and early diagnosis. Stud Health Technol Inform. 2005;117:51–9.
4. Suri JS, Kathuria C, Molinari F. Atherosclerosis disease management. Springer; 2011
5. • Boesen ME, Singh D, Menon BK, Frayne R. A systematic literature review of the effect of carotid atherosclerosis on local vessel stiffness and elasticity. Atherosclerosis. 2015;243:211–22. **This article exhibits the effect of carotid atherosclerotic plaque on local arterial stiffness**.
6. Gamble G, Zorn J, Sanders G, MacMahon S, Sharpe N. Estimation of arterial stiffness, compliance, and distensibility from M-mode ultrasound measurements of the common carotid artery. Stroke. 1994;25:11–6.
7. Lechareas S, Yanni A, Golemati S, Chatziioannou A, Perrea D. Ultrasound and biochemical diagnostic tools for the characterization of vulnerable carotid atherosclerotic plaque. Ultrasound Med Biol. 2015;42:31–43.
8. Yuan LJ, Xue D, Duan YY, Coa TS, Yang HG, Zhou N. Carotid arterial intima–media thickness and arterial stiffness in pre-

eclampsia: analysis with a radiofrequency Ultrasound technique. Ultrasound Obstet Gynecol. 2013;42:644–52.
9. Zhang L, Yin JK, Duan YY, Liu X, Xu L, Wang J, et al. Evaluation of carotid artery elasticity changes in patients with type 2 diabetes. Cardiovasc Diabetol. 2014;13:1–10.
10. Bianchini E, Gemignani V, Faita F, Giannarelli C, Ghiadoni L, Demi M, et al. Assessment of carotid stiffness and intima-media thickness from ultrasound data: comparison between two methods. J Ultrasound Med. 2010;29:1169–75.
11. Blacher J, Asmar R, Djane S, London GM, Safar ME. Aortic pulse wave velocity as a marker of cardiovascular risk in hypertensive patients. Hypertension. 1999;33:1111–7.
12. Mattace-Raso FUS, van der Cammen TJM, Hofman A, van Popele NM, Bos ML, Schalekamp MADH, et al. Arterial stiffness and risk of coronary heart disease and stroke: the Rotterdam study. Circulation. 2006;113:657–63.
13. Greenwald SE. Pulse pressure and arterial elasticity. Q J Med. 2002;95:107–12.
14. Antonini-Canterin F, Roşca M, Beladan CC, Popescu BA, Piazza R, Leiballi E, et al. Echo-tracking assessment of carotid artery stiffness in patients with aortic valve stenosis. Echocardiography. 2009;26:823–31.
15. Gimbrone Jr MA, Cybulsky MI, Kume N, Collins T, Resnick N. Vascular endothelium: an integrator of pathophysiological stimuli in atherogenesis. Ann N Y Acad Sci. 1995;748:122–31.
16. Hansson GK, Libby P, Tabas I. Inflammation and plaque vulnerability. J Intern Med. 2015;278:483–93.
17. Ross R. Cell Biology of atherosclerosis. Annu Rev Physiol. 1995;57:791–804.
18. Tabas I, Williams KJ, Borén J. Subendothelial lipoprotein retention as the initiating process in atherosclerosis: update and therapeutic implications. Circulation. 2007;116:1832–44.
19. Luthra K, Mishra A, Srivastava LM. Lipoprotein(a): biology and role in atherosclerotic vascular diseases. Curr Sci. 1999;76:1553–60.
20.•• Libby P, Ridker PM PM, Hansson GK. Progress and challenges in translating the biology of atherosclerosis. Nature. 2011;473:317–25. **This article discusses the pathophysiological formation of the atherosclerotic plaque**.
21. Raines EW, Ferri N. Thematic review series: the immune system and atherogenesis, cytokines affecting endothelial and smooth muscle cells in vascular disease. J Lipid Res. 2005;46:1081–92.
22. Arroyo LH, Lee RT. Mechanisms of plaque rupture: mechanical and biologic interactions. Cardiovasc Res. 1999;41:369–75.
23. Teng Z, Zhang Y, Huang Y, Feng J, Yuan J, Lu Q, et al. Material properties of components in human carotid atherosclerotic plaques: a uniaxial extension study. Acta Biomater. 2014;10:5055–63.
24. Cohn JN, Colucci W. Cardiovascular effects of aldosterone and post-acute myocardial infarction pathophysiology. Am J Cardiol. 2006;97:4–12.
25. Tracqui P, Broisat A, Toczek J, Mesnier N, Ohayon J, Riou L. Mapping elasticity moduli of atherosclerotic plaque in situ via atomic force microscopy. J Struct Biol. 2011;174:115–23.
26. Geng YJ, Libby P. Evidence for apoptosis in advanced human atheroma: co-localization with interleukin-1-converting enzyme. Am J Pathol. 1995;147:251–66.
27. Isner JM, Kearney M, Bortman S, Passeri J. Apoptosis in human atherosclerosis and restenosis. Circulation. 1995;91:2703–11.
28. Geng YJ, Wu Q, Muszynski M, Libby P. Apoptosis of vascular smooth muscle cells induced by in vitro stimulation with interferon-gamma, tumor necrosis factor-alpha, and interleukin-1-beta. Arterioscler Thromb Vasc Biol. 1996;16:19–27.
29. Bruel A, Oxlund H. Changes in biomechanical properties, composition of collagen and elastin, and advanced glycation endproducts of the rat aorta in relation to age. Atherosclerosis. 1996;127:155–65.
30. Cheung YF, Wong SJ, Ho MH. Relationship between carotid intima-media thickness and arterial stiffness in children after Kawasaki disease. Arch Dis Child. 2007;92:43–7.
31. Cheung YF, Chow PC, Chan GC, Ha SY. Carotid intima media thickness is increased and related to arterial stiffening in patients with beta-thalassaemiamajor. Br J Haematol. 2006;135:732–34.
32. Zhang L, Yin JK, Duan YY, Liu X, Xu L, Wang J, et al. Evaluation of carotid artery elasticity changes in patients with type 2 diabetes. Cardiovasc Diabetol. 2014. doi:10.1186/1475-2840-13-39.
33.•• Selzer RH, Mack WJ, Lee PL, Kwong-Fu H, Hodis HN. Improved common carotid elasticity and intima-media thickness measurements from computer analysis of sequential ultrasound frames. Atherosclerosis. 2011;154:185–93. **The article uses computerized edge tracking method for carotid arterial diameter and carotid intima-media thickness measurement in multiple frames of the cardiac cycle**.
34. Avolio AP, Chen SG, Wang RP, Zhang CL, Li MF, O'Rourke MF. Effects of aging on changing arterial compliance and left ventricular load in a northern Chinese urban community. Circulation. 1983;68:50–8.
35. Huang X, Kang X, Xue J, Kang C, Lv H, Li Z. Evaluation of carotid artery elasticity changes in patients with cerebral small vessel disease. Int J Clin Exp Med. 2015;8:18825–30.
36. Laurent S, Katsahian S, Fassot C, Tropeano AI, Gautier I, Laloux B, et al. Aortic stiffness is an independent predictor of fatal stroke in essential hypertension. Stroke. 2003;34:1203–6.
37. Callaghan FJ, Geddes LA, Babba CF, Bourland JD. Relationship between pulse-wave velocity and arterial elasticity. Med Biol Eng Comput. 1986;24:248–54.
38. Soleimani E, Mokhtari-Dizaji M, Saberi H. A novel non-invasive ultrasonic method to assess total axial stress of the common carotid wall in healthy and atherosclerotic men. J Biomech. 2015;48:1860–7.
39. Meaume S, Benetos A, Henry OF. Aortic pulse wave velocity predicts cardiovascular mortality in subjects >70 years of age. Arterioscler Thromb Vasc Biol. 2001;21:2046–50.
40. Farrar DJ, Green HD, Bond MG, Wagner WD, Gobbeé RA. Aortic pulse wave velocity, elasticity, and composition in a nonhuman primate model of atherosclerosis. Circ Res. 1978;43:52–62.
41. Cinthio M, Ahlgren AR, Bergkvist J, Jansson T, Persson HW, Lindström K. Longitudinal movements and resulting shear strain of the arterial wall. Am J Physiol Heart Circ Physiol. 2006;291:394–402.
42. Svedlund S, Gan LM. Longitudinal wall motion of the common carotid artery can be assessed by velocity vector imaging. Clin Physiol Funct Imaging. 2011;31:32–8.
43. Oates CP, Naylor AR, Hartshorne T, Charles SM, Fail T, Humphries K, et al. Joint recommendations for reporting carotid ultrasound investigations in the United Kingdom. Eur J Vasc Endovasc Surg. 2009;37:251–61.
44. Wong CB, Wong JC. A novel method to quantify carotid artery stenosis by Doppler ultrasound: Using the continuity principle. Int J Angiol. 2010;19:86–90.
45. Shapiro GL, Stockman CG. Computer Vision. 1st ed. Pearson; 2000.
46. Destrempes F, Meunier J, Giroux MF, Soulez G, Cloutier G. Segmentation in ultrasonic B-mode images of healthy carotid arteries using mixtures of nakagami distributions and stochastic optimization. IEEE Trans Med Imaging. 2009;28:215–29.
47. Haas C, Ermert H, Holt S, Grewe P, Machraoui A, Barmeyer J. Segmentation of 3-D intravascular ultrasonic images based on a random field model. Ultrasound Med Biol. 2000;26:297–306.
48. Francois O. Global optimization with exploration/selection algorithms and simulated annealing. Ann Appl Probab. 2002;12:248–71.

49. Molinari F, Zeng G, Suri JS. An integrated approach to computer-based automated tracing and its validation for 200 common carotid arterial wall ultrasound images: a new technique. J Ultrasound Med. 2010;29:399–418.
50. Seabra JC, Ciompi F, Pujol O, Mauri J, Radeva P, Sanches J. Rayleigh mixture model for plaque characterization in intravascular ultrasound. IEEE Trans Biomed Eng. 2011;58:1314–24.
51. Menchon-Lara RM, Bastida-Jumilla MC, Morales-Sanchez J, Sancho-Gomez JL. Automatic detection of the intima-media thickness in ultrasound images of the common carotid artery using neural networks. Med Biol Eng Comput. 2014;52:169–81.
52. Carvalho DDB, Akkus Z, Van den Oord SCH, Schinkel AFL, Van der Steen AFW, Niessen WJ, et al. Lumen segmentation and motion estimation in B-mode and contrast-enhanced ultrasound images of the carotid artery in patients with atherosclerotic plaque. IEEE Trans Med Imaging. 2015;34:883–93.
53. Jayaram S, Esakkirajan S, Veerakumar T. Digital image processing. 1st ed. Tata McGraw-Hill Education; 2009.
54. Kass M, Witkin A, Terzopoulos D. Snakes: active contours models. Int J Comput Vis. 1988;4:321–31.
55. Suri JS, Farah A. Deformable models volumes I and II: biomedical and clinical applications (Topics in biomedical engineering). 1st ed. Springer; 2007.
56. Loizou CP, Pattichis CS, Pantziaris M, Tyllis T, Nicolaides A. Snakes based segmentation of the common carotid artery intima media. Med Biol Eng Comput. 2007;45:35–49.
57. Molinari F, Meiburger KM, Zeng G, Nicolaides A, Suri JS. CAUDLES-EF: carotid automated ultrasound double line extraction system using edge flow. J Digit Imaging. 2011;24:1059–77.
58. Golemati S, Stoitsis J, Sifakis EG, Balkizas T, Nikita KS. Using the Hough transform to segment ultrasound images of longitudinal and transverse sections of the carotid artery. Ultrasound Med Biol. 2007;33:918–32.
59. Liang Q, Wendelhag I, Wikstrand J, Gustavsson T. A multiscale dynamic programming procedure for boundary detection in ultrasonic artery images. IEEE Trans Med Imaging. 2000;19:127–42.
60. Meiburger KM, Molinari F, Acharya UR, Saba L, Rodrigues P, Liboni W, et al. Automated carotid artery intima layer regional segmentation. Phys Med Biol. 2011;56:4073–90.
61. Ilea DE, Duffy C, Kavanagh L, Stanton A, Whelan PF. Fully automated segmentation and tracking of the intima media thickness in ultrasound video sequences of the common carotid artery. IEEE Trans Ultrason Ferroelectr Freq Control. 2013;60:158–77.
62. Kanber B, Ramnarine KV. A probabilistic approach to computerized tracking of arterial walls in ultrasound image sequences. Int Sch Res Netw (ISRN). 2012. doi:10.5402/2012/179087.
63. Chen Y, Peng B, Liu DC. Fully automated intima media thickness measurement of posterior wall in longitudinal ultrasound B-mode scans. Int J Signal Process Image Process Pattern Recog. 2014;7:9–18.
64. Touboul PJ, Prati P, Scarabin PY, Adrai V, Thibout E, Ducimetiere P. Use of monitoring software to improve the measurement of carotid wall thickness by B-mode imaging. J Hypertens. 1992;10:37–41.
65. Molinari F, Meiburger KM, Zeng G, Acharya UR, Liboni W, Nicolaides A, et al. Carotid artery recognition system: a comparison of three automated paradigms for ultrasound images. Med Phys. 2012;39:378–91.
66.• Molinari F, Zeng G, Suri JS. A state of the art review on intima-media thickness (IMT) measurement and wall segmentation techniques for carotid ultrasound. Comput Methods Prog Biomed. 2010;100:201–21. **The paper presents review different methods for lumen-intima and mediaadventitia boundary segmentation techniques such as: dynamic programming, local statistics, edge-detection, active contours, statistical modelling, Hough transform, and hybrid techniques. It also discusses about carotid IMT measurement techniques**.
67. Meiburger KM, Molinari F, Zeng G, Saba L, Suri JS. Carotid automated ultrasound double line extraction system (CADLES) via Edge-Flow. Conf Proc IEEE Eng Med Biol Soc. 2011. doi:10.1109/IEMBS.2011.6090107.
68. Suri JS. Computer vision, pattern recognition and image processing in left ventricle segmentation: the last 50 years. Pattern Anal Applic. 2000;3:209–42.
69. El-Baz A, Gimel'farb D, Suri JS. Stochastic modeling for medical image analysis. 1st ed. CRC Press; 2015.
70. Molinari F, Meiburger KM, Acharya UR, Zeng G, Rodrigues PS, Saba L, et al. CARES 3.0: a two stage system combining feature-based recognition and edge-based segmentation for CIMT measurement on a multi-instititional ultrasound database of 300 images. Conf Proc IEEE Eng Med Biol Soc. 2011. doi:10.1109/IEMBS.2011.6091275.
71. Hassan M, Chaudhry A, Khan A, Iftikhar MA. Robust information gain based fuzzy c-means clustering and classification of carotid artery ultrasound images. Comput Methods Prog Biomed. 2014;113:593–609.
72. Rocha R, Campilho A, Silva J, Azevedo E, Santos R. Segmentation of ultrasound images of the carotid using RANSAC and cubic splines. Comput Methods Prog Biomed. 2011;101:94–106.
73. Yamagishi T, Kato M, Koiwa Y, Hasegawa H, Kanai H. Impact of lifestyle-related diseases on carotid arterial wall elasticity as evaluated by an ultrasonic phased-tracking method in Japanese subjects. J Med Ultrason. 2009;16:782–92.
74. Araki T, Ikeda N, Dey N, Chakraborty S, Saba L, Kumar D, et al. A comparative approach of four different image registration techniques for quantitative assessment of coronaryartery calcium lesions using intravascular ultrasound. Comput Methods Prog Biomed. 2015;118:158–72.
75. Zhang P, Guo R, Xiao D, Chu S, Gong L, Zhang C, et al. Influence of smoking cessation on carotid artery wall elasticity evaluated by echo-tracking. J Clin Ultrasound. 2012;40:352–6.
76. Apostolakis IZ, Gastounioti A, Golemati S, Nikita KS. Ultrasound-image-based displacement and strain maps of the human carotid artery using weighted-least-squares optical flow. IEEE Int Conf Imaging Syst Tech (IST). 2012. doi:10.1109/IST.2012.6295565.
77. Saba L, Molinari F, Meiburger KM, Piga M, Zeng G, Rajendra Achraya U, et al. What is the correct distance measurement metric when measuring carotid ultrasound intima-media thickness automatically? Int Angiol. 2012;31:483–9.
78. Molinari F, Meiburger KM, Zeng G, Saba L, Rajendra Acharya U, Famiglietti L, et al. Automated carotid IMT measurement and its validation in low contrast ultrasound database of 885 patient Indian population epidemiological study: results of AtheroEdge™ Software. Int Angiol. 2012;31:42–53.
79. Huttenlocher DP, Klanderman GA, Rucklidge WJ. Comparing images using the Hausdorff distance. IEEE Trans Pattern Anal Mach Intell. 1993;15:850–63.
80. Thacher T, Gambillara V, da Silva RF, Silacci P, Stergiopulos N. Reduced cyclic stretch, endothelial dysfunction, and oxidative stress: an ex vivo model. Cardiovasc Pathol. 2010;19:91–8.
81. Palombo C, Kozakova M. Arterial stiffness, atherosclerosis and cardiovascular risk: pathophysiologic mechanisms and emerging clinical indications. Vasc Pharmacol. 2015;15:332–68.
82. Cardoso L, Kelly-Arnold A, Maldonado N, Laudier D, Weinbaum S. Effect of the tissue properties, shape and orientation of micro calcification on vulnerable cap stability using different hyperelastic constitutive models. J Biomech. 2014;47:870–7.
83. Gronholdt ML, Nordestgaard BG, Bentzon J, Wiebe BM, Zhou J, Falk E, et al. Macrophages are associated with lipid-rich carotid artery plaques, echolucency on B-mode imaging, and elevated plasma lipid levels. J Vasc Surg. 2002;35:137–45.

84. Packard RRS, Libby P. Inflammation in atherosclerosis: from vascular biology to biomarker discovery and risk prediction. Clin Chem. 2008;54:24–38.
85. Sehgel NL, Sun Z, Hong Z, Hunter WC, Hill MA, Vatner DE, et al. Augmented vascular smooth muscle cell stiffness and adhesion when hypertension is superimposed on aging. Hypertension. 2015;65:370–7.
86. Pahkala K, Hernelahti M, Heinonen OJ, Raittinen P, Hakanen M, Lagström H, et al. Body mass index, fitness and physical activity from childhood through adolescence. Br J Sports Med. 2013;47:71–7.
87. Cecelja M, Chowienczyk P. Dissociation of aortic pulse wave velocity with risk factors for cardiovascular disease other than hypertension: a systematic review. Hypertension. 2009;54:1328–36.
88. Miyamoto M, Kotani K, Okada K, Ando A, Hasegawa H, Kanai H, et al. Arterial wall elasticity measured using the phased tracking method and atherosclerotic risk factors in patients with type 2 diabetes. J Atheroscler Thromb. 2013;20:678–87.
89.• Laurent S, Boutouyrie P, Lacolley P. Structural and genetic bases of arterial stiffness. Hypertension. 2005;45:1050–5. **The paper talks about biological factors responsible for arterial stiffness. This change in stiffness has association with the genetic components**.
90. Mahmud A, Feely J. Effect of smoking on arterial stiffness and pulse pressure amplification. Hypertension. 2003;41:183–7.
91. Simons PC, Algra A, Bots ML, Grobbee DE, van der Graaf Y. Common carotid intima-media thickness and arterial stiffness indicators of cardiovascular risk in high-risk patients. Circulation. 1999;100:951–7.
92. Zahnd G, Orkisz M, Sérusclat A, Moulin P, Vray D. Simultaneous extraction of carotid artery intima-media interfacesin ultrasound images: assessment of wall thickness temporal variation during the cardiac cycle. Int J CARS. 2014;9:645–58.
93. Niu L, Qian M, Song R, Meng L, Liu X, Zheng H. A texture matching method considering geometric transformations in noninvasive ultrasonic measurement of arterial elasticity. Ultrasound Med Biol. 2012;38:524–33.
94. Hasegawa H, Kanai H, Hoshimiya N, Koiwa Y. Evaluating the regional elastic modulus of a cylindrical shell with nonuniform wall thickness. J Med Ultrason. 2004;31:81–90.
95. Pahkala K, Laitinen TT, Heinonen J, Viikari JSA, Rönnemaa T, Niinikoski H, et al. Association of fitness with vascular intima-media thickness and elasticity in adolescence. Pediatrics. 2013;132:77–84.
96. Mitchell GF, Hwang SJ, Vasan RS, Larson MG, Pencina MJ, Hamburg NM, et al. Arterial stiffness and cardiovascular events: the Framingham Heart Study. Circulation. 2010;4:505–11.
97. Saba L, Meiburger KM, Molinari F, Ledda G, Anzidei M, Acharya UR, et al. Carotid IMT variability (IMTV) and its validation in symptomatic versus asymptomatic Italian population: can this be a useful index for studying symptomaticity? Echocardiography. 2012;29(9):1111–9.
98. Saba L, Banchhor SK, Suri HS, Londhe ND, Araki T, Ikeda N, et al. Accurate cloud-based smart IMT measurement, its validation and stroke risk stratification in carotid ultrasound: a web-based point-of-care tool for multicenter clinical trial. Comput Biol Med. 2016;75:217–34.